Journal of Electron Spectroscopy and Related Phenomena, 28 (1982) 149—170
Elsevier Scientific Publishing Company, Amsterdam — Printed in The Netherlands

CORE-HOLE SPECTRA OF D^+—Ar—A^- MOLECULES IN THE SOLID STATE (D = DIALKYLAMINO; A = PYRIDINIUM, PYRYLIUM, THIAPYRYLIUM)

R. W. BIGELOW and R. J. WEAGLEY

Xerox Webster Research Center, Webster, NY 14580 (U.S.A.)

H.-J. FREUND

Lehrstuhl für Theoretische Chemie der Universität zu Koln, 5000 Cologne 41 (W. Germany)

(First received 20 November 1981; in final form 26 June 1982)

ABSTRACT

Solid-state XPS spectra of selected D^+—Ar—A^- molecular systems bearing a pyridinium, pyrylium or thiapyrylium fragment as the acceptor (A^-) and the dialkylamino group as the common donor (D^+) are presented and analyzed on the basis of CNDO/S—CI equivalent-core computations for model compounds. The acceptor characteristics of the pyridinium, pyrylium and thiapyrylium substituents are compared to those of the nitro group in *p*-nitroaniline. Clearly resolved, intense shake-up excitations (~ 20% of the main peak intensity) are associated with N 1*s* donor ionization in the pyrylium and thiapyrylium derivatives, whereas heteroatomic ionization in the acceptor group yields shake-up intensities of 20—30%. Unlike the case for *p*-nitroaniline, however, the response of the valence electrons to ionization provides little screening of the core hole, leading to relatively intense satellites well separated from the main peaks. Also, the orbitals of interest appear sufficiently shielded due to steric factors so as to inhibit core-hole-induced intermolecular interactions. Heteroatomic binding-energy differences (ΔBE) in accordance with experiment are extracted from charge-potential calculations. Analysis of the intra- and inter-molecular contributions to the relative chemical shifts shows ΔBE to be a sensitive function of the ion/counter-ion pairing scheme.

INTRODUCTION

Considerable attention has recently been given to the origin of the intense multipeak structure observed in the core-hole spectra of organic D^+—Ar—A^- molecules in both the gas phase and solid state [1—17]. Numerous recent studies have attributed such intense satellite features or multipeak structure to $D^+ \rightarrow A^-$ valence-orbital $\pi^* \leftarrow \pi$ excitations accompanying creation of the core hole [2—17]. Both the intensity and separation of the satellites

0368-2048/82/0000—0000/$02.75

from the main peak have been shown to be a sensitive function of orbital localization. In the case of vapor-phase N 1*s* core-hole ionization of the *p*-nitroaniline nitro group, for example, shake-up states appear within ~ 1.0 eV of the primary ionization [12—14]. In addition, Domcke and co-workers [10,11] have pointed out similarities between the origin of the multipeak core-hole spectra of *p*-nitroaniline and the dynamic screening of adsorbate core holes by charge transfer from the substrate.

The purpose of this work is to extend our study of D^+—Ar—A^- core-hole spectra to include compounds where the acceptor moiety is defined by an extended conjugated system containing a carbon skeleton with a heteroatom as an XPS probe. The systems under study can be compared with *N,N*-dialkylamino-*p*-nitroaniline where the nitro group is replaced with a pyridinium, pyrylium or thiapyrylium fragment. These substituents constitute *closed-shell* cations, and as such are strong electron acceptors. In particular, we examine the condensed-phase XPS spectra (see Fig. 1) of (1) *trans-N*-methyl-4(4′-dimethylaminostyryl)pyridinium methylsulfate (DASP/$CH_3SO_4^-$), (2) 2,6-diphenyl-4(4′-diethylaminophenyl)pyrylium tetrafluoroborate (DPDEAPP/BF_4^-), and (3) 2,6-diphenyl-4(4′-diethylaminophenyl) thiapyrylium tetrafluoroborate (DPDEAPT/BF_4^-).

The results of CNDO/S—CI equivalent-core computations for DASP and a model DPDEAPP compound permit both the acceptor *and* donor broad/multipeak heteroatomic core-hole spectra shown in Fig. 1 to be resolved into primary ionization and shake-up contributions. Explicit counterion contributions to the molecular potential yield relative binding-energy differences in accordance with experiment.

EXPERIMENTAL

XPS measurements were conducted using an AEI ES200B photoelectron spectrometer (normal operating pressure ~ 10^{-8} torr). Photoelectron spectra of DASP/$CH_3SO_4^-$ were accumulated using an unfiltered Mg $K\alpha$ source ($\hbar\omega = 1253.7$ eV), whereas spectra of DPDEAPP/BF_4^- and DPDEAPT/BF_4^- were obtained using an unfiltered Al $K\alpha$ source ($\hbar\omega = 1486.7$ eV). All samples were mounted in powder form directly onto the probe tip by means of double-sided tape.

COMPUTATIONAL

Explicit computations for the core-hole species and accompanying core-hole-excited states for the molecules of interest here are likely to be not only very costly, but quite sensitive to truncation of the basis set. With these difficulties in mind we rely on suitable approximations to examine

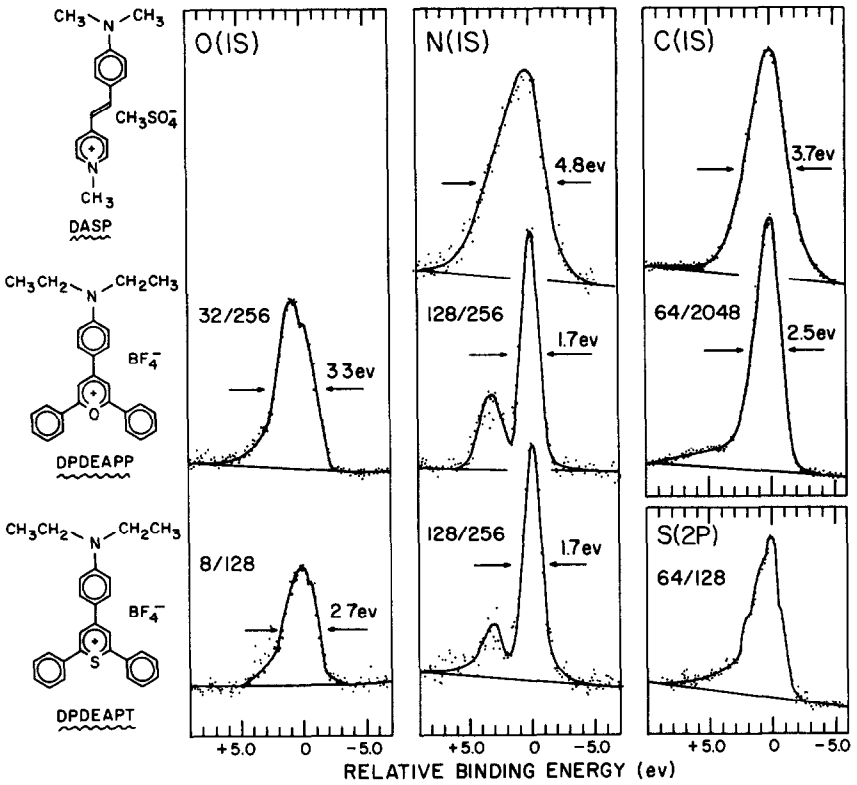

Fig. 1. XPS spectra of DASP/$CH_3SO_4^-$, DPDEAPP/BF_4^- and DPDEAPT/BF_4^-. The DASP O1*s* and DPDEAPT C1*s* spectra were not recorded in detail. The number of scans, *S*, and the multichannel-analyzer scale factor *SF* are given opposite the pyrylium and thiapyrylium spectra (*S*/*SF*).

the nature of the perturbations to the valence-orbital manifold due to the creation of a localized core hole. Quantum chemical computations were, therefore, performed within the closed-shell CNDO/S—CI framework [18,19] using the Nishimoto—Mataga approximation to the two-center electron—electron interaction integrals [20]. The equivalent-core approximation [21,22] was used to simulate the effects of selected core holes by replacing the atom to be ionized (atomic number Z) by the next highest atom in the periodic table ($Z' = Z + 1$) and performing calculations of the originally closed-shell system as a closed-shell system with charge one unit greater. Depending on whether the counterion is included, the net charge on the resulting initial species will be zero (cation plus counterion) or + 1e (cation). The CNDO/S method has been parametrized specifically to yield neutral-molecule excitation energies of first-row conjugated organic systems ($Z \leqslant 10$) within a limited configuration-interaction space, and we expect this technique, subject to the equivalent-core constraint, to be also well-suited to describe

charge-relaxation effects due to the creation of a localized core hole. Previous applications of this approach, *with emphasis on large organic systems*, support this viewpoint [9,13—17]. Although the excited states of our partly relaxed hole-state $(Z+1)$ calculation remain classified in terms of singlet and triplet parentage, we rely on establishing an *equivalence* between the *average* configuration energy for the states of interest calculated within the $(Z+1)$ description and the corresponding average configuration energy of the actual ionic system in order that the calculated values be appropriate to the final hole-state species. A limited-configuration-interaction calculation between the 60 lowest-energy singly excited configurations was performed to indicate the "purity" of the final ionic states. In all cases considered it was found that the final-state wavefunctions of interest were composed almost entirely of the simple one-electron excitation from the highest occupied π molecular orbital (HOMO) to the lowest unoccupied π molecular orbital (LUMO).

In terms of the initial N-electron closed-shell molecule, an electronic excitation from orbital ϕ_i to orbital ϕ_j leads to one-electron singlet and triplet configurations having energies [23] given by

$$^1\tilde{E}_{ij'}(N) = \epsilon_{j'} - \epsilon_i - J_{ij'} + 2K_{ij'} \tag{1a}$$

and

$$^3\tilde{E}_{ij'}(N) = \epsilon_{j'} - \epsilon_i - J_{ij'} \tag{1b}$$

where ϵ_i and $\epsilon_{j'}$ are the occupied and virtual Hartree—Fock orbital energies, and $J_{ij'}$ and $K_{ij'}$ are the Coulomb and exchange integrals, respectively. Ionization of a core orbital ϕ_k leads to the $(N-1)$-electron, 1-spin, Koopmans' core-hole doublet state $(^2\tilde{E}^0(k) = -\epsilon_k)$, the $m_s = 1/2$ component being

$$^2\Phi^0(k) = |\phi_k\phi_i\bar{\phi}_i| \tag{2}$$

whereas valence-orbital excitation in the presence of the core hole leads to a 3-spin, two-hole—one-particle (2h—1p) system from which two doublet states and one quartet state arise [24,25], the $m_s = 1/2$ components of which are

$$^2\Phi^1(k) = 2^{-1/2}\{|\phi_k\bar{\phi}_i\phi_{j'}| - |\phi_k\phi_i\bar{\phi}_{j'}|\} \tag{3a}$$

$$^2\Phi^3(k) = 6^{-1/2}\{2|\bar{\phi}_k\phi_i\phi_{j'}| - |\phi_k\bar{\phi}_i\phi_{j'}| - |\phi_k\phi_i\bar{\phi}_{j'}|\} \tag{3b}$$

$$^4\Phi(k) = 3^{-1/2}\{|\phi_k\phi_i\bar{\phi}_{j'}| + |\phi_k\bar{\phi}_i\phi_{j'}| + |\bar{\phi}_k\phi_i\phi_{j'}|\} \tag{3c}$$

$^2\Phi^1(k)$ is termed the "singlet"-coupled doublet, whereas $^2\Phi^3(k)$ is denoted the "triplet"-coupled doublet to reflect the relative projections of the valence-electron spins [26]. Within the basis set of the unperturbed mole-

cule, ${}^1\Psi^0(N)$, the $(N-1)$-electron 2h—1p energies are given ($\epsilon_k = 0$) [24,27] by

$$ {}^2\tilde{E}^1_{ij'}(k) = [(\epsilon_{j'} - J_{j'k}) - (\epsilon_i - J_{ik}) - J_{ij'}] + 2K_{ij'} - 1/2K_{ik} + 1/2K_{j'k} \quad (4a) $$

$$ {}^2\tilde{E}^3_{ij'}(k) = [(\epsilon_{j'} - J_{j'k}) - (\epsilon_i - J_{ik}) - J_{ij'}] + 1/2K_{ik} + 3/2K_{j'k} \quad (4b) $$

$$ {}^4\tilde{E}_{ij'}(k) = [(\epsilon_{j'} - J_{j'k}) - (\epsilon_i - J_{ik}) - J_{ij'}] - K_{ik} \quad (4c) $$

where the terms have been arranged to provide maximum coincidence with corresponding elements for the closed-shell system. Comparison of eqns. (1) and (4) readily verifies that the valence-orbital excitation energies for the closed-shell molecule can be significantly perturbed by the core hole depending on the magnitude of the core—valence-electron Coulomb and exchange coupling. Selective interactions are dramatically demonstrated in the case of *p*-nitroaniline [10,13,14]. It should be emphasized that the energy expressions of eqn. (4) are relative to the ground state. Although K_{ik} and $K_{j'k}$ contribute equally in the expression for the *total* 2h—1p energies, subtraction of ${}^1\tilde{E}^0(N)$, which has no $K_{j'k}$ contribution, causes the core—valence exchange integrals to appear in the final terms with unequal coefficients. K_{ik} and $K_{j'k}$ do, however, appear with equal coefficients in the 2h—1p energies derived from open-shell relaxed hole-state calculations [28,29].

As noted previously [10,13,14], the terms in parentheses in eqn. (4) can be viewed as electrostatic shifts of the neutral-molecule orbital eigenvalues due to the core hole. Although the $(Z+1)$equivalent-core approach directly approximates $J_{j'k}$ and J_{ik} by modifying the effective nuclear charge of the center to be ionized [21,22], excitation energies are still rendered in terms of singlet and triplet character. The excitation energies of the $(Z+1)$ system can then be expressed as

$$ {}^1\tilde{E}_{ij'}(Z+1) = [(\epsilon_{j'} - J_{j'k}) - (\epsilon_i - J_{ik}) - J_{ij'}] + 2K_{ij'} \quad (5a) $$

and

$$ {}^3\tilde{E}_{ij'}(Z+1) = [(\epsilon_{j'} - J_{j'k}) - (\epsilon_i - J_{ik}) - J_{ij'}] \quad (5b) $$

where $\epsilon_{j'} - J_{j'k}$ and $\epsilon_i - J_{ik}$ are approximations to the $(Z+1)$-system eigenvalues. Owing to the mixed valence spin character of the 2h—1p wavefunctions, we rely on establishing an equivalence between the average configuration energies to extract meaningful 2h—1p multiplet splittings from the results of the $(Z+1)$ calculations. We assume, therefore, that ${}^{1,3}\tilde{E}^{\mathrm{AVG}}_{ij'}$ $(Z+1)$ represents some partly relaxed (correlated) 2h—1p configuration. The average configuration energies from eqns. (4) and (5), where $\tilde{A}$ is the quantity in square brackets, are

$$ {}^{1,3}\tilde{E}^{\mathrm{AVG}}_{ij'}\ (Z+1) = \tilde{A} + 1/2K_{ij'} \quad (6) $$

$$^{2,4}\tilde{E}_{ij'}^{\mathrm{AVG}}(k) = \tilde{A} + 1/2K_{ij'} + 1/2K_{j'k} - 1/2K_{ik} \tag{7}$$

Rather than assuming an equivalence between $^{1,3}\tilde{E}_{ij'}^{\mathrm{AVG}}(Z+1)$ and $^{2,4}\tilde{E}_{ij'}^{\mathrm{AVG}}(k)$ as proposed originally [13,14], we now substitute into eqn. (7) only those terms calculated directly, i.e., $\tilde{A} + 1/2K_{ij'}$. Combining eqns. (4), (6) and (7) yields

$$^{2}\tilde{E}_{ij'}^{1}(k) = {}^{1,3}\tilde{E}_{ij'}^{\mathrm{AVG}}(Z+1) + 3/2K_{ij'} + 1/2K_{j'k} - 1/2K_{ik} \tag{8}$$

$$^{2}\tilde{E}_{ij'}^{3}(k) = {}^{1,3}\tilde{E}_{ij'}^{\mathrm{AVG}}(Z+1) - 1/2K_{ij'} + 3/2K_{j'k} + 1/2K_{ik} \tag{9}$$

$$^{4}\tilde{E}_{ij'}(k) = {}^{1,3}\tilde{E}_{ij'}^{\mathrm{AVG}}(Z+1) - 1/2K_{ij'} - K_{ik} \tag{10}$$

To maintain a direct connection with the 2h—1p basis set we elect to evaluate the exchange terms appearing in eqns. (8)–(10) on the basis of the relative orbital localizations in the neutral molecule. $K_{ij'}$ is, of course, the valence—valence exchange term evaluated in the neutral—molecule problem, whereas $K_{j'k}$, for example, is

$$\begin{aligned} K_{j'k} &= \langle \phi_{1s}(1)\phi_{j'}(2)|r_{12}^{-1}|\phi_{1s}(2)\phi_{j'}(1)\rangle \\ &\approx C_{1s}^2 C_{j'}^2 \langle \chi_{1s}(1)\chi_{j'}(2)|r_{12}^{-1}|\chi_{1s}(2)\chi_{j'}(1)\rangle \end{aligned} \tag{11}$$

where the term in brackets is confined to atomic orbitals χ on the same center, and C_{1s} and $C_{j'}$ are the LCAO coefficients. In accordance with our earlier work, this term is given a value of ~ 1.2 eV [30]. In the case of a completely localized core hole,

$$K_{j'k} \simeq 1.2C_{j'}^2 \tag{12}$$

and

$$K_{ik} \simeq 1.2C_i^2 \tag{13}$$

In our original approach to establish a relationship which could be used to extract reasonable ionic 2h—1p multiplet energies from a$(Z+1)$ calculation [13,14], we used the doublet-state energies given by Domcke and co-workers [10], which differ from those of the present study in the coefficients $K_{ij'}$ and K_{ik}, and in the quartet-state energy given by eqn. (4c). The present approximation, eqns. (8)—(10), is based on a consistent definition of terms which yields 2h—1p excitation energies for *p*-nitroaniline closely paralleling those of our earlier work [13,14]. Generally, $^{2}\tilde{E}_{ij'}^{1}(k)$ is reduced by only several tenths of an eV, whereas $^{2}\tilde{E}_{ij'}^{3}(k)$ is increased by approximately this amount. Values previously calculated for *p*-nitroaniline can, therefore, be compared directly with the results of this study. Furthermore, our original interpretation as to the origin of the differences between the vapor- and condensed-phase XPS spectra of *p*-nitroaniline is unchanged [13,14].

Shake-up intensities are given within the sudden approximation in terms of initial (N) and final-state ($N-1$) determinantal wavefunctions [31, 32]

by

$$^2I^1_{ij'}(k) = |\langle ^2\Psi^F_{ij'}(N-1)|\,^1\Psi^G(N)\rangle|^2 \tag{14}$$

Previous computational studies of the heteroatomic core-hole ionization of large organic D^+—Ar—A^- systems have revealed that the *primary* source of deviation from orthogonality between $^2\Psi^F_{ij'}(N-1)$ and $^1\Psi^G(N)$ is mixing between the HOMO and LUMO levels, and that such mixing can lead to relatively intense, low-energy, single-component shake-up excitations [9—11, 13—17]. Rather than attempting to calculate absolute values, we here pursue a simplistic approach and rationalize the experimental satellite features contained in Fig.1 in terms of relative intensities extracted from a specific subset of orbitals including the four highest occupied and the LUMO π levels. Within this approach the exact expression for the relative intensities

$$^2I^1_{ij'}(k)/^2I_0(k) = |\langle ^2\Psi^F_{ij'}(N-1)|\,^1\Psi^G(N)\rangle|^2 / |\langle ^2\Psi^F_0(N-1)|\,^1\Psi^G(N)\rangle|^2 \tag{15}$$

is approximated as

$$^2I_{ij'}(k)/^2I_0(k) = (\bar{f}/f)\,|\langle D^{Z+1}_{ij'}(\tilde{\pi})|D^N(\pi)\rangle|^2 / |\langle D^{Z+1}(\tilde{\pi})|D^N(\pi)\rangle|^2 \tag{16}$$

where $\langle D^{Z+1}(\tilde{\pi})|D^N(\pi)\rangle$ is the determinantal overlap formed between the selected subset of occupied orbitals, and $\langle D^{Z+1}_{ij'}(\tilde{\pi})|\,D^N(\pi)\rangle$ is the overlap formed by replacing an orbital ϕ_i in the occupied subset by the LUMO level $\phi_{j'}$. Owing to higher-lying shake-up and shake-off processes, $\bar{f}$ and f may be considerably less than unity [33—35]. For the purposes of this analysis we assume $\bar{f}/f = \bar{w} = 1$.

Within our approximation, $^2I^3_{ij'}(k) \equiv 0$ [34]. It is well known, however, that "triplet"-coupled doublet excitations can gain intensity through *secondary* interaction with either the primary core-hole state or "singlet"-coupled doublet excitations [30,36]. Owing to the relatively large shake-up energies encountered in this study, coupling between the relaxed 2h—1p states and the primary core hole is assumed to be negligible. Furthermore, assuming that the only significant coupling between spin manifolds is likely to occur between excitations involving the same spatial orbitals, the matrix element of interest becomes (within the basis set of the neutral molecule) [27]

$$\langle ^2\Phi^1_{\pi\pi^*}(k)|H|\,^2\Phi^3_{\pi\pi^*}(k)\rangle = 3/\sqrt{12}\,(K_{\pi k} - K_{\pi^* k}) \tag{17}$$

In accordance with the preceding arguments, the cross-coupling term reduces to

$$H^{1,3}_{\pi\pi^*}(k) \simeq 1.039\,(C^2_{\pi} - C^2_{\pi^*}) \tag{18}$$

where, again, C_{π} and C_{π^*} represent the single valence-orbital LCAO coefficient of the ionized center. Using the relationship

$$H^{1,3}_{\pi\pi^*}(k) \simeq \Delta^2 \tilde{E}^{1,3}_{\pi\pi^*}(k) \tag{19}$$

as a criterion for efficient cross-coupling, it is found that owing to the delocalized nature of the orbitals of interest neither C_{π} or C_{π^*} is of sufficient magnitude to promote a splitting likely to be resolvable experimentally. Explicit computation verifies this expectation, and we therefore neglect interactions between spin manifolds.

Atomic coordinates for the isolated molecules were derived from our earlier work [15,37,38]. For DASP we considered only the *trans* configuration (planar π structure) and an alternating single—double—single bond linkage between aromatic chromophores, of 1.46—1.34—1.46 Å, respectively. Since the basis-set requirements for DPDEAPP exceed our program limitations we used 2,6-dimethyl-4(4′-dimethylaminophenyl)pyrylium (DMDMAPP) as a model electronic system and considered both a "quinoid" and an "aromatic" geometry [37,38] Also, since our version of CNDO/S is limited to elements having $Z \leqslant 10$ computations for the corresponding thiapyrylium analog were not possible. Counterion bonding effects were examined by including an appropriate counterion (BF_4^-) directly in the SCF procedure [37,38].

RESULTS AND DISCUSSION

DASP

Figure 2 and Table 1 show that according to our computations DASP can be grouped within the classification of a D^+—Ar—A^- system, with the dimethylaminophenyl group (DAP) approximating the D^+—Ar— component (HOMO localized on DAP at −10.69eV) and the remaining pyridinium fragment (Py) assuming the —A^- character (LUMO localized on Py at − 5.35eV). In the *N*-electron-system ground state, the *N*-methylpyridinium fragment withdraws (accepts) only 0.180e of charge from the D^+—Ar— groups, compared to 0.351e withdrawn by the nitro group in *p*-nitroaniline (PNA) [14]. The large positive charge remaining on the Py fragment is associated with the carbon centers, rather than the heteroatom [38]. In accordance with the usual characterization of D^+—Ar—A^- systems, HOMO → LUMO optical excitation occurs at relatively low energies ($^1\tilde{E}_{\pi\pi^*}(N) = 3.05$eV), is strongly dipole-allowed ($f \simeq 1.0$), and is accompanied by considerable charge transfer from the D^+—Ar— moieties (Δq = 0.702e). In comparison, charge-transfer excitation in PNA yields a $\Delta q(D^+ —Ar \rightarrow NO_2)$ of 0.595e [39], indicating that while the nitro group has a

TABLE 1

CALCULATED HOMO → LUMO EXCITATION PROPERTIES FOR DASP, DMDMAPP (Q) AND DMDMAPP(A) ISOLATED CATIONS[a]

	DASP			DMDMAPP(Q)			DMDMAPP(A)		
Property	Initial	N_{Py} 1s(A)	N_{DAP} 1s(D)	Initial	O 1s(A)	N 1s(D)	Initial	O 1s(A)	N 1s(D)
ϵ_{π^*}(LUMO)	−5.34	−9.46	−7.40	−5.34	−9.14	−8.43	−5.50	−9.97	−8.00
ϵ_{π}(HOMO)	−10.69	−13.28	−14.15	−11.42	−14.70	−15.00	−11.64	−14.48	−15.67
$\Delta\epsilon_{\pi\pi^*}$	5.35	3.82	6.75	6.08	5.56	6.57	6.14	4.51	7.67
$^1\tilde{E}_{\pi\pi^*}$	3.05	2.25	3.97	3.35	3.33	3.81	3.60	2.67	4.66
$^3\tilde{E}_{\pi\pi^*}$	2.23	0.42	2.41	2.13	1.33	1.96	2.66	0.95	2.98
$f(^1\tilde{E}_{\pi\pi^*})$	0.9997			1.4107			0.8788		
Δq $D^+ - Ar \rightarrow A^-$	0.702	0.440	0.488	0.288	0.109	0.085	0.617	0.496	0.425
Δq $N \rightarrow Ar - A^-$	0.237	0.250	0.031	0.126	0.103	0.010	0.284	0.384	0.018
$^{1,3}\tilde{E}^{AVG}_{\pi\pi^*}$	2.43	0.88	2.80	2.44	1.83	2.42	2.90	1.38	3.40
$K_{\pi\pi^*}$	0.41	0.92	0.78	0.61	1.00	0.93	0.47	0.86	0.84
$C_{\pi k}$ A^-	0.126	−0.120	0.213	0.182	0.104	−0.193	0.107	0.076	−0.164
$C_{\pi k}$ D^+	−0.493	0.530	−0.122	0.415	0.447	−0.162	0.603	0.658	−0.143
$C_{\pi^* k}$ A^-	0.407	−0.203	0.385	0.210	−0.101	−0.194	0.283	0.133	0.261
$C_{\pi^* k}$ D^+	0.067	−0.165	0.044	−0.223	0.275	0.114	−0.097	−0.194	0.052

[a] Quantities not previously defined in the text include the oscillator strength f and the magnitude of charge transfer (Δq) to or from the indicated moieties concomitant with excitation. Energies are in electronvolts and the excitation energies include *slight* depressions from the one-electron HOMO → LUMO values due to configuration interaction.

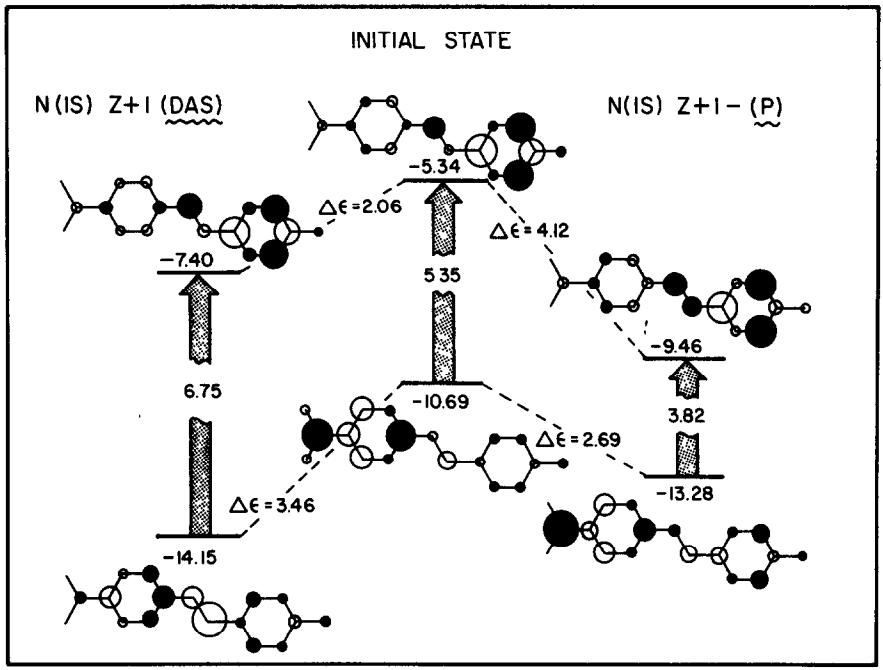

Fig. 2. Schematic view from above molecular plane of initial and $(Z+1)$ ionized DASP HOMO and LUMO orbitals (eV). The orbital lobes are drawn proportional to the LCAO coefficients.

stronger influence on the ground-state properties, the Py substituent is a more efficient excited-state acceptor. Cursory examinations of explicit counterion bonding were conducted by including BF_4^- directly in the computational scheme and calculating the structure as a supermolecule [14,38]. Such counterion bonding yielded negligible perturbations to the intramolecular properties of current interest. The manifestations of counterion bonding are considered in detail below.

Table 2 shows that core-hole ionization of the *acceptor* pyridinium nitrogen, N_{Py} 1*s*, yields two relatively intense shake-up states within 4.0eV of the primary core-hole emission. $^2\Psi_1^1(k)$ is clearly attributable to HOMO $\rightarrow$ LUMO excitation, whereas most of the intensity contained in the higher-lying $^2\Psi_2^1(k)\pi^* \leftarrow \pi$ excitation is derived from ground-state correlation effects (see discussion in following Section). Two approximately compensating differences between the electronic structures of DASP and PNA serve to rationalize the similar calculated shake-up energies for N1*s acceptor* ionization ($^2\tilde{E}^1_{\pi\pi^*}(k) = 1.36$eV) for PNA [14]. First, the LUMO level of DASP is $\sim$ 2.0eV lower in energy than that calculated for PNA, implying that if 2h 1p interactions were similar in the two systems the DASP shake-up energies would be much lower than those calculated for PNA. Second,

TABLE 2
VARIOUS TERMS OF CHARGE-POTENTIAL MODEL DERIVED FROM ISOLATED CATION USED TO ADDRESS CORE-HOLE BINDING-ENERGY DIFFERENCES

Term	Donor		Acceptor	
	DASP	DMDMAPP[a]	DASP	DMDMAPP[a]
Q_i^0(e)	−0.227	−0.173	−0.048	−0.169
Q_i^+(e)	+0.077	+0.087	+0.144	+0.196
Σ_i^0(e)	+4.384	+5.712	+6.530	+6.590
Σ_i^+(e)	+8.358	+9.275	+9.721	+8.166
E_i^{REL}(eV)	−5.635	−4.902	−3.900	−5.168

[a] Values for DMDMAPP refer to the quinoid configuration.

delocalization of the DASP LUMO acceptor orbital onto the carbon centers surrounding the nitrogen atom yields J_{π^*k}(DASP) $< J_{\pi^*k}$(PNA). In the case of acceptor ionization $J_{\pi^*k} \gg J_{\pi k}$ has been identified as the primary source for the strong stabilization of D^+—Ar—$A^-\pi^* \leftarrow \pi$ singlet excitations relative to the neutral species [5,10,11,13—16].

Figure 2 also indicates that the 2h—1p excitations do not provide additional screening directly to the site of ionization as in the case of PNA [14]. It is interesting to note, however, that valence-orbital rearrangement in response to the creation of the N_{Py} 1*s* *primary core hole* is such that 80% of the core-hole charge is neutralized, yielding relative carbon/nitrogen charge-density differences similar to those for the *N*-electron structure. The shake-up states, therefore, do significantly enhance screening of the *relaxed* core-hole-state centers of greatest positive charge (Fig. 2), i.e., the carbon centers adjacent to the ionized center.

N_{DAP}1*s* donor ionization yields ${}^2\tilde{E}^{\frac{1}{1}}(k) = 3.927$eV and ${}^2\tilde{E}^{\frac{1}{2}}(k) = 5.653$eV relative to ${}^2\tilde{E}^0(k) = 0$. The shift of the 2h—1p $\pi^* \leftarrow \pi$ excitations to higher energy relative to the *N*-electron system is clearly attributable to $J_{\pi k} > J_{\pi^*k}$ for acceptor ionization. Owing to the relative orbital localizations, however, these shifts are less severe than those calculated for PNA [14]. Also, in accordance with our results for PNA, donor ionization is found to yield only weak shake-up features.

Our resolution of the broad, asymmetric single-peak N_{DASP}1*s* emission is given in Fig. 3 assuming a binding-energy difference ΔBE_{ij} between N_{Py} 1*s* and N_{DAP}1*s* of 2.0eV, and $f(N_{Py}1s)/f(N_{DAP}1s) \simeq 1.0$. Manifestations of selective intra- and inter-molecular (counterion) contributions which account for $\Delta BE_{ij} \simeq 2.0$eV can be clearly defined in terms of the charge-potential model including differential relaxation [30,40—42]:

$$\Delta BE_{ij} = K\Delta Q_{ij}^0 + \Delta\Sigma_{ij}^0 + \Delta E_{ij}^{REL} \qquad (20)$$

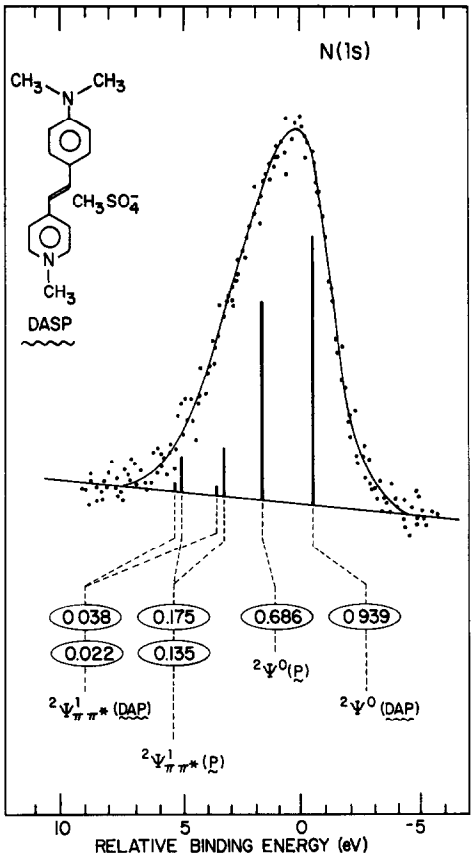

Fig. 3. DASP N1*s* solid-state photoionization spectrum resolved into primary core-hole, $^2\Psi^0(k)$, and shake-up, $^2\Psi^1_{\pi\pi^*}(k)$, contributions, assuming an $(N_{Py}1s)$—$(N_{DAP}1s)$ binding-energy difference of ≈ 2.0 eV.

where, relative to the N-electron configuration, ΔQ^0_{ij} is the difference in net atomic charge, $\Delta\Sigma^0_{ij}$ is the difference in molecular potential given by

$$\Delta\Sigma^0_{ij} = \sum_{k \neq i} (Q^0_i R^{-1}_{ik}) - \sum_{k \neq j} (Q^0_j R^{-1}_{jk}) \tag{21}$$

(R being the interatomic separation), and $K = 24.0\,\mathrm{eVe}^{-1}$ for the CNDO/S parametrization [14]. The relaxation-energy contribution ΔE^{REL}_{ij} represents the average difference of the charge-potential terms calculated in the fields of the N-electron (0) and relaxed ($Z + 1$) configurations (+) [41], i.e.,

$$\Delta E^{REL}_{ij} = 1/2[(K\Delta Q^0_{ij} + \Delta\Sigma^0_{ij}) - (K\Delta Q^+_{ij} + \Delta\Sigma^+_{ij})] \tag{22}$$

For the case of an ion pair, DASP—$CH_3SO_4^-$ for example, the terms arising from the molecular potential ($\Delta\Sigma_{ij}$) can be divided into parts due only

to the cation (C) (*intramolecular*) and anion (A) (*intermolecular*) charge centers:

$$\Delta\Sigma^{0}_{ij} = \Delta\Sigma^{0(C)}_{ij} + \Delta\Sigma^{0(A)}_{ij} \tag{23}$$

and

$$\Delta\Sigma^{+}_{ij} = \Delta\Sigma^{+(C)}_{ij} + \Delta\Sigma^{+(A)}_{ij} \tag{24}$$

Furthermore, the assumption of negligible polarization of the anion charge concomitant with the creation of the core hole, as reflected by our computations, yields

$$\Delta\Sigma^{0(A)}_{ij} = \Delta\Sigma^{+(A)}_{ij} \tag{25}$$

For computational convenience, eqn. (20) can be rearranged in the form

$$\Delta BE_{ij} = 1/2[K(3\Delta Q^{0}_{ij} + \Delta Q^{+}_{ij}) + 3\Delta\Sigma^{0(C)}_{ij} - \Delta\Sigma^{+(C)}_{ij}] + \Delta\Sigma^{0(A)}_{ij} \tag{26}$$

The counterion therefore causes only an electrostatic shift in ΔBE_{ij} calculated in the absence of the external charge center(s). Substitution of the values from Table 3 for the "isolated" DASP cation into eqn. (26) yields

$$\Delta BE[(N_{DAP}1s)\cdots(N_{Py}1s)] = -8.18 + \Delta\Sigma^{0(A)}_{ij} \tag{27}$$

TABLE 3

LOW-LYING CORE-HOLE EXCITATION ENERGIES, RELEVANT CROSS-COUPLING MATRIX ELEMENTS AND INTENSITY RATIOS OF INTEREST[a]

	DASP		DMDMAPP(Q)		DMDMAPP(A)	
	$N_{Py}1s$(A)	$N_{DAP}1s$(D)	O1s(A)	N1s(D)	O1s(A)	N1s(D)
$^2\tilde{E}^1_1$(eV)	1.898	3.932	3.036	3.471	2.129	4.472
$^2\tilde{E}^1_2$(eV)	3.709	5.653	5.284	5.773	4.617	7.940
$^2\tilde{E}^3_1$(eV)	1.296	3.409	1.909	2.523	1.688	4.031
$^2\tilde{E}^3_2$(eV)	3.249	4.597	4.471	5.338	3.395	6.718
$H^{1,3}_1$(eV)	−0.155	0.248	−0.011	0.127	−0.071	0.368
$H^{1,3}_2$(eV)	−0.120	0.254	−0.005	0.292	−0.063	0.336
$^2I^1_1/^2I_0$	0.261	0.040	0.247	0.150 (0.212)	0.243	0.051
$^2I^1_2/^2I_0$	0.196	0.023	0.071	0.094 (0.028)	0.066	0.027

[a] $^2\Psi^{1,3}_1(k)$ and $^2\Psi^{1,3}_2(k)$ are, respectively, the *one-electron* HOMO → LUMO excitation and the next lowest-lying excitation to the LUMO level having non-negligible intensity. The slight amount of configuration interaction contained in the excitation energies of Table 1 is neglected here. The values in parentheses were obtained from the adjusted determinantal overlap as described in the text.

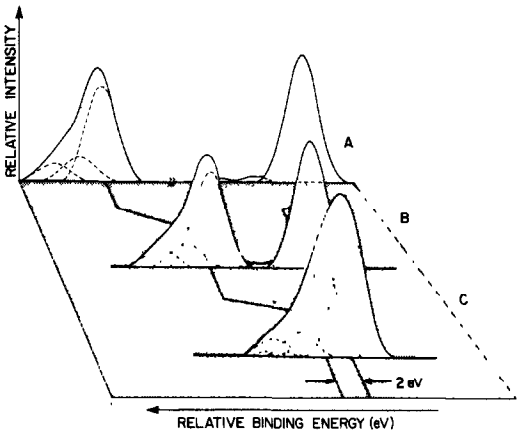

Fig. 4. Theoretical DASP N1*s* core-hole spectrum at various levels of approximation: (a) "uncorrelated" spectrum; the $N_{Py}1s$ component is placed at the higher binding energy to reflect the relative atomic charges on the nitrogen atoms (Table 2); (b) spectrum obtained in accordance with the charge-potential model, assuming negligible counterion contributions; and (c) spectrum obtained by including the counterion in the charge-potential model opposite the cation fragment of greatest positive charge.

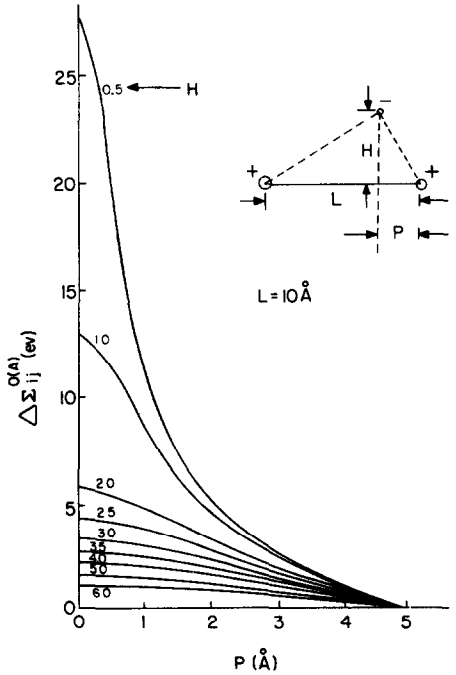

Fig. 5. Contributions to molecular potential assuming indicated cation/anion pairing scheme. P is the counterion—$N_{Py}1s$ separation projected onto the molecular plane. P can of course assume negative values, for which $\Delta\Sigma_{ij}^{0(A)}$ remains positive. In the case that $P > 5.0$ Å, $\Delta\Sigma_{ij}^{0(A)}$ becomes negative, thereby enhancing the $(N_{Py}1s)$—$(N_{DAP}1s)$ splitting which is not observed experimentally.

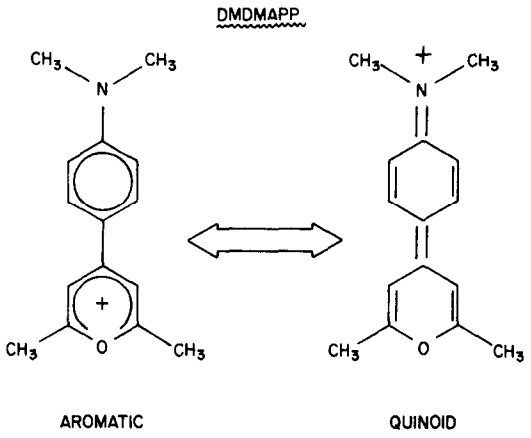

Fig. 6. Aromatic and quinoid DMDMAPP molecular configurations used to model electronic properties of DPDEAPP and DPDEAPT.

Neglect of the anion contributions clearly results in a splitting greater than the experimental value by ~ 6.0eV (Fig. 4)! Figure 5 indicates, assuming (a) an experimental splitting of $\leqslant 2.0$eV, (b) interaction with a single, point charge, and (c) reasonable values of the cation—anion separation, that in order to achieve $\Delta\Sigma_{ij}^{0(A)} \simeq 6.0$eV the anion must lie preferentially adjacent to N_{Py}. The close proximity of N_{Py} to the counterion suggested by Fig. 5 is not surprising, since 0.702e of the charge of the N-electron closed-shell cation is localized on the acceptor fragment. Lu and co-workers [43] have, in fact, confirmed such a preferential counterion bonding scheme for DASP paired with I^-.

The apparent agreement between experiment and the computations implies a small or negligible intermolecular orbital overlap between adjacent DASP moieties, unlike the situation encountered for condensed-phase PNA [14]. The DASP molecular orbitals of interest (Fig. 2) appear well shielded from such considerations, owing to steric factors.

DPDEAPP and DPDEAPT

Figure 1 shows clearly resolved secondary features associated with the narrow, well-defined N1*s* *donor* core-hole emissions of DPDEAPP and DPDEAPT (~ 3.1eV above the main peak, with $I \simeq 28\%$ and 19%, respectively). Like DASP, the pyrylium and thiapyrylium fragments assume an acceptor character. As noted above, owing to computational limitations we performed N-electron and $(Z + 1)$ calculations for the model compound DMDMAPP assuming an "aromatic" (A) and a "quinoid" (Q) geometry (Fig. 6) as a means of addressing the manifestations of both acceptor and donor core-hole ionization in DPDEAPP and DPDEAPT. The quinoid configuration was included in this study to reflect contributions to the solid-state structure such as determined experimentally for DPDEAPT/

ClO_4^- (BF_4^-) by Dulmage and co-workers [44]. The N-electron ground- and excited-state properties of DMDMAPP have been discussed in detail elsewhere [38]. Briefly, it is found that while the aromatic configuration appears necessary to achieve HOMO/LUMO localization within the conventional $D^+ - Ar - A^-$ scheme, as reflected by the magnitude of intramolecular charge transfer given in Table 1, shake-up intensities (Table 2) arising from the aromatic configuration parallel those calculated for PNA and DASP; i.e., a large intensity is associated with the acceptor heteroatom ionization, whereas a small or negligible intensity appears concomitant with N1s donor ionization. This situation, particularly in regard to donor ionization, is clearly at odds with experiment (Fig. 1). The extended conjugation imparted by the quinoid structure (Fig. 7) yields low-energy N1s donor shake-up excitations three times more intense than those obtained from the aromatic geometry, and thus better approximates experiment. In addition, the shake-up excitation energy $^2\tilde{E}_1^1$ calculated for DMDMAPP(Q) appears in closer accordance with experiment than the value extracted from the localized aromatic configuration ($^2\tilde{E}^1_{\pi\pi^*}(k) = 3.471\,\text{eV}$ versus $^2\tilde{E}^1_{\pi\pi^*}(k) = 4.472\,\text{eV}$).

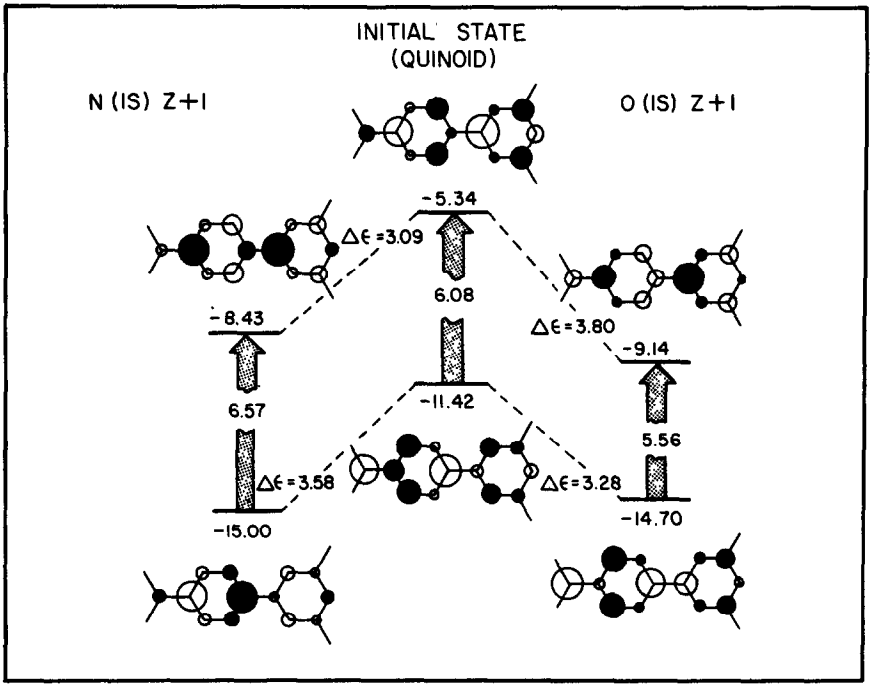

Fig. 7. Schematic view from above molecular plane of initial and $(Z+1)$ ionized DMDMAPP(Q) HOMO and LUMO orbitals (eV). The orbital lobes are drawn proportional to the LCAO coefficients.

TABLE 4
PORTION OF DETERMINANTAL OVERLAP USED TO ADDRESS N1*s* SHAKE-UP INTENSITIES OF DMDMAPP(Q)

	$\tilde{\pi}_{H-3}$	$\tilde{\pi}_{H-2}$	$\tilde{\pi}_{H-1}$	$\tilde{\pi}_{HOMO}$	$\tilde{\pi}_{LUMO}$
π_{H-3}	0.974	0	0	0	0
π_{H-2}	0	0.850	0	−0.481	0.058
π_{H-1}	0	0	0.937	0	0
π_{HOMO}	0	−0.196	0	−0.896	−0.288

As in the case of DASP, for DMDMAPP(Q) the relatively strong $^2\Psi_2^1$(N1*s*) excitation gains intensity at the expense of $^2\Psi_1^1$(N1*s*) through "secondary" coupling terms in the determinantal overlap—"ground-state correlation" contributions (in the nomenclature of Martin and Shirley [45]), rather than a single-orbital overlap factor which establishes the parentage. From Table 4 the overlap appropriate for $^2\Psi_1^1(k)$ excitation reduces to

$$\langle D_1^{Z+1}(\tilde{\pi})|D^N(\pi)\rangle \simeq \langle\tilde{\pi}_{H-2}|\pi_{H-2}\rangle\langle\tilde{\pi}_{LUMO}|\pi_{HOMO}\rangle - \langle\tilde{\pi}_{LUMO}|\pi_{H-2}\rangle\langle\tilde{\pi}_{H-2}|\pi_{HOMO}\rangle \quad (28)$$

The first product gives -0.245, whereas the second term enters with a positive phase factor ($+0.011$) yielding $\langle D_1^{Z+1}(\tilde{\pi})|D^N(\pi)\rangle = -0.234$. Integration over spin variables gives $^2I_1^1 \simeq 0.109$ compared to $^2I_1^1 \simeq 0.165$ obtained assuming simple $\tilde{\pi}_{LUMO}$—π_{HOMO} overlap. Similar considerations for $^2\Psi_2^1(k)$ yield $^2I_2^1 \simeq 0.073$ from the contracted determinantal overlap, compared to $^2I_2^1 \simeq 0.007$ obtained assuming only $\tilde{\pi}_{LUMO}$—π_{H-2} overlap. This discrepancy between the computed spectrum and experiment can be rationalized by noting the probable perturbations induced by replacing the 2,6-methyl groups of the model compound by phenyl moieties to yield a species more in accordance with that actually measured. It has been shown [37] for model compounds that 2,6-diphenyl substitution of the pyrylium cation yields orbitals with eigenvalues approximately midway between those of the π_{HOMO} and π_{H-2} levels. For the purposes of argument we assume that such substitution destabilizes the π_{HOMO} by 0.5eV, whereas π_{H-2} is stabilized by this amount. Furthermore, assuming that the off-diagonal elements of the determinantal overlap are inversely proportional to the orbital eigenvalue difference, an adjusted (A) determinantal overlap can be generated from the initial value (I):

$$\langle\tilde{\pi}_i|\pi_j\rangle_A \simeq \langle\tilde{\pi}_i|\pi_j\rangle_I (\Delta\epsilon_{ij}^I/\Delta\epsilon_{ij}^A) \quad (29)$$

where the diagonal elements are normalized according to

$$\langle\tilde{\pi}_i|\pi_i\rangle_A \simeq \langle\tilde{\pi}_i|\pi_i\rangle_I + [\langle\tilde{\pi}_i|\pi_j\rangle_I(1-\Delta\epsilon_{ij}^I/\Delta\epsilon_{ij}^A)]^2 \quad (30)$$

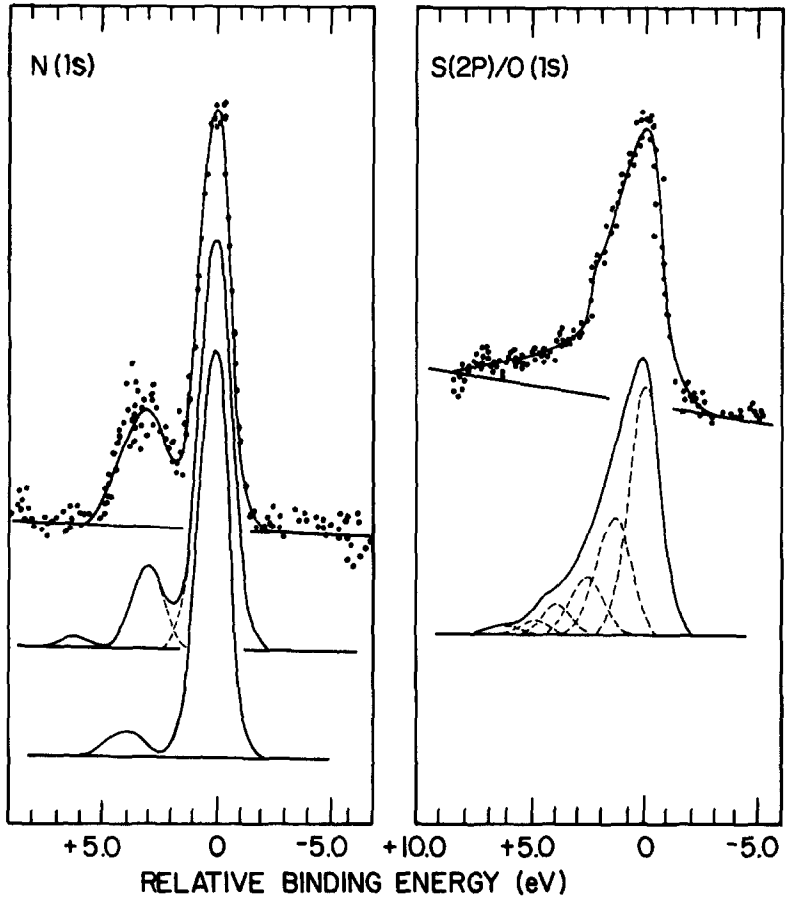

Fig. 8. Comparison of experimental N1*s* core-hole spectrum of DPDEAPP with theoretical DMDMAPP spectrum obtained using both quinoid *adjusted* and aromatic geometries, and of experimental S2*p* core-hole spectrum of DPDEAPT with theoretical O1*s* spectrum of DMDMAPP(Q) adjusted as described in the text.

Such an analysis serves to decrease the magnitude of the off-diagonal terms enhancing ${}^2I_1^1/{}^2I_0$ at the expense of ${}^2I_2^1/{}^2I_0$. Intensity ratios obtained in accordance with these arguments are given in Table 3. The DMDMAPP(Q) adjusted N1*s* core-hole spectrum is compared with experiment and with the values obtained from the aromatic configuration in the left-hand panel of Fig. 8.

Comparisons of the DPDEAPP and DPDEAPT acceptor ionizations with computations for DMDMAPP pose some difficulty. First, the O1*s* signal of DPDEAPP is 3→4 times stronger than that anticipated on the basis of the 1:1 oxygen:nitrogen atomic ratio and the relative Scofield photoemission cross-sections (σ(O1*s*) = 2.85; σ(N1*s*) = 1.78) [46]. Second, the O1*s* signal

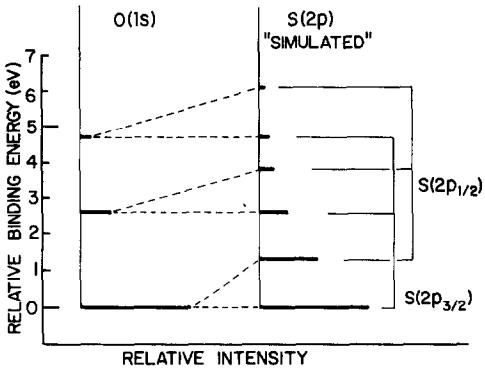

Fig. 9. Decomposition of theoretical DMDMAPP(Q) O1*s* shake-up spectrum into components assumed to simulate the S2*p* spectrum of DPDEAPT.

arising from DPDEAPP is similar in structure (resolution), intensity and binding energy to the O1*s* spectrum of the thiapyrylium analog, which has no inherent oxygen component. The O1*s* emissions in Fig. 1 are, therefore, attributed to oxygen contaminants. Insight into the acceptor core-hole ionization process can nevertheless be achieved by comparing the computation for O1*s* ionization of DMDMAPP with the experimental S2*p* spectrum of DPDEAPT, which apparently does not suffer from contaminant contributions. The S2*p* spectrum, however, is a spin—orbit-split doublet, $\Delta E(S2p_{1/2,3/2}) = 1.3$eV [30], with relative photoemission cross-sections of $\sigma(S2p_{1/2}) = 0.590$ and $\sigma(S2p_{3/2}) = 1.155$ [46]. The simulated S2*p* spectrum is constructed from the computations for O1*s* ionization of DMDMAPP by first partitioning the primary intensity into two independent emissions consistent with the relative cross-sections and separated by 1.3eV. Computed shake-up energies and intensities are then referenced separately to the parent components, as shown in Fig. 9. The right-hand panel of Fig. 8 compares the constructed S2*p* spectrum with experiment using the results for the quinoid geometry. As indicated in Table 3, the shake-up intensity derived from acceptor ionization does not appear to be sensitive to the geometry changes considered.

As in the case of DASP, the relative orbital localizations (Fig. 7) inhibit the acceptor core hole from strongly stabilizing, or the donor core hole from destabilizing, the shake-up excitation relative to the corresponding neutral-molecule excitation.

Figure 1 and our analysis of the core-hole spectrum of DASP indicate that the N1*s* *donor* binding energy of DASP is approximately equal to that of DPDEAPP and DPDEAPT. This correspondence and eqn. (26) allow the relative intra- and inter-molecular (counterion) contributions to N1*s* core-hole relaxation arising from two dissimilar chemical environments to be expressed in a particularly simple form. Substitution of the intramolecular terms from Table 2 for donor ionization of DASP, $N_i 1s$, and DMDMAPP(Q), $N_j 1s$, into eqn. (26) yields

$$\Delta BE_{ij} = -3.60 + \Delta\Sigma_{ij}^{0(A)} \quad (31)$$

Thus, in order to achieve the equivalence between the binding energies of the N1*s* levels that is observed experimentally ($\Delta BE_{ij} \simeq 0$), Fig. 5 indicates that the counterion must be in closer proximity to the donor group of DMDMAPP than in the case of DASP. This conclusion is consistent with the findings of Dulmage and co-workers [44] which locate the DPDEAPT counterion approximately midway between the thiapyrylium and D^+—Ar— fragments, and the results of Lu et al. [43] which confirm a distinctly preferential pyridinium/counterion pairing in DASP.

SUMMARY AND CONCLUSIONS

This study has demonstrated that the broad/multipeak heteroatomic XPS spectra of selected pyridinium, pyrylium and thiapyrylium molecules in the solid state can be elucidated in terms of selective electrostatic counterion bonding and processes inherent to core-hole ionization. The particular systems addressed have been modeled in accordance with the results of CNDO/S—CI equivalent-core computations and discussed within the framework of D^+—Ar—A^- configurations, with the pyridinium, pyrylium and thiapyrylium moieties as the acceptors and the dialkylamino group as the common donor. Systematic analysis of these systems has revealed both similarities and significant differences with respect to previous work on the widely studied D^+—Ar—A^- system, *p*-nitroaniline.

In particular, it is concluded that for the systems described here shake-up processes provide little screening of the core hole, leading to relatively intense satellites well separated from the main peak. A "quinoid" character or extended conjugation between the pyrylium or thiapyrylium fragments and the remaining parts of the respective molecules is suggested, indicating that a classification of these systems in terms of D^+—Ar—A^- character is less well defined than in the case of the pyridinium compound, where the interacting moieties are separated by an alternating single—double—single bond linkage. In addition, the computations have been shown to reflect the significantly different counterion pairing schemes observed experimentally for the pyridinium and thiapyrylium (pyrylium) derivatives.

Finally, the finding that the computations for the isolated cations, subject to electrostatic binding-energy shifts due to the counterion, reflect the solid-state shake-up spectra supports our previous interpretation of the differences between the vapor- and condensed-phase XPS spectra observed for *p*-nitroaniline; i.e., whereas the *p*-nitroaniline orbitals of interest are well localized at the extremities of the molecule so as to promote intermolecular overlap, those of the pyridinium, pyrylium and thiapyrylium derivatives appear well shielded from such considerations, owing to steric factors.

ACKNOWLEDGMENTS

We thank G.R. Meredith and R.F. Ziolo for making us aware of the work of Lu and co-workers (ref. 43).

REFERENCES

1 K. Siegbahn, C. Nordling, A. Fahlman, R. Nordberg, K. Hamrin, J. Hedman, G. Johansson, T. Bergmark, S.-E. Karlsson, I. Lindgren and B. Lindberg, ESCA: atomic, molecular and solid state structure studied by means of electron spectroscopy, Nova Acta Reg. Soc. Sci. Ups., Ser. IV, 20 (1967).
2 S. Pignataro and G. Distefano, J. Electron Spectrosc. Relat. Phenom., 2 (1973) 171.
3 S. Pignataro, R. DiMarino and G. Distefano, J. Electron Spectrosc. Relat. Phenom., 4 (1974) 90.
4 S. Pignataro and G. Distefano, Z. Naturforsch., 30a (1975) 815.
5 G. Distefano, D. Jones, A. Modelli and S. Pignataro, Phys. Scr., 16 (1977) 373.
6 S. Tsuchiya and M. Seno, Chem. Phys. Lett., 54 (1978) 132.
7 A. Randino and F. Battaglia, J. Electron Spectrosc. Relat. Phenom., 20 (1980) 327.
8 R. Nakagaki, D. C. Frost and C. A. McDowell, J. Electron Spectrosc. Relat. Phenom., 19 (1980) 355.
9 G. Distefano, M. Guerra, D. Jones, A. Modelli and F. P. Colonna, Chem. Phys., 52 (1980) 389.
10 W. Domcke, L. S. Cederbaum, J. Schirmer and W. von Niessen, Phys. Rev. Lett., 42 (1979) 1237; Chem. Phys., 39 (1979) 149.
11 W. Domcke, J. Schirmer and W. von Niessen, Phys. Scr., 21 (1980) 481.
12 M. S. Banna, Chem. Phys., 45 (1980) 383.
13 R. W. Bigelow and H.-J. Freund, Chem. Phys. Lett., 77 (1981) 261.
14 H.-J. Freund and R. W. Bigelow, Chem. Phys., 55 (1981) 407.
15 R.W. Bigelow, R. J. Weagley and H.-J. Freund, Chem. Phys. Lett., 82 (1981) 305.
16 R. W. Bigelow, M. S. Banna, H.-J. Freund, H. Lex and H. Deger, J. Chem. Phys., in preparation.
17 R. W. Bigelow and H.-J. Freund, J. Chem. Phys., submitted for publication.
18 J. E. DelBene, H. H. Jaffé, R. L. Ellis and G. Kuehnlenz, QCPE Vol. 10 (1974) 174, Quantum Chemistry Program Exchange, Bloomington, IN.
19 R. L. Ellis, G. Kuehnlenz and H. H. Jaffé, Theor. Chim. Acta, 26 (1972) 131.
20 K. Nishimoto and N. Mataga, Z. Phys. Chem. (Frankfurt), 12 (1957) 335.
21 W. L. Jolly and D. N. Hendrickson, J. Am. Chem. Soc., 92 (1970) 1863.
22 L. J. Aarons, M. F. Guest and I. H. Hillier, J. Chem. Soc., Faraday Trans. 2, 68 (1972) 1866.
23 C. C. J. Roothaan, Rev. Mod. Phys., 23 (1951) 69.
24 F. L. Pilar, Elementary Quantum Chemistry, McGraw—Hill, New York, 1968.
25 S. P. McGlynn, L. G. Vanquickenborne, M. Kinoshita and D. G. Carroll, Introduction to Applied Quantum Chemistry, Holt, Rinehart and Winston, New York, 1972.
26 H. Basch, Chem. Phys., 10 (1975) 157.
27 M. F. Guest, I. H. Hillier, V. R. Saunders and M. H. Wood, Proc. R. Soc. (London), Ser. A, 333(1973) 201.
28 D. A. Lowitz, J. Chem. Phys., 46 (1967) 4698.
29 R. Zahradnik and P. Carsky, J. Phys. Chem., 74 (1970) 1235.

30 K. Siegbahn, C. Nordling, G. Johansson, J. Hedman, P. R. Heden, K. Hamrin, U. Gelius, T. Bergmark, L. O. Werne, R. Manne and Y. Baer, ESCA Applied to Free Molecules, North-Holland, Amsterdam, 1969.
31 T. Åberg, Ann. Acad. Sci. Fenn., Ser. AVI, 308 (1969) 7.
32 R. Manne and T. Åberg, Chem. Phys. Lett., 7 (1970) 282.
33 P. S. Bagus, M. Schrenk, D. W. Davis and D. A. Shirley, Phys. Rev. A, 9(1974) 1090.
34 T. Darko, I. H. Hillier and J. Kendrick, Mol. Phys., 32 (1976) 33.
35 H.-J. Freund, E. W. Plummer, W. R. Salaneck and R. W. Bigelow, J. Chem. Phys., 75 (1981) 4275, and references cited therein.
36 T. X. Carroll and T. D. Thomas, J. Electron Spectrosc. Relat. Phenom., 10 (1977) 215.
37 R. W. Bigelow, J. Chem. Phys., 67 (1977) 4498.
38 R. W. Bigelow, J. Chem. Phys., 73 (1980) 3864.
39 R. W. Bigelow, H.-J. Freund and B. Dick, Theor. Chim. Acta, submitted for publication.
40 U. Gelius, Phys. Scr., 9 (1974) 133.
41 L. Hedin and A. Johansson, J. Phys. B, 2 (1969) 1336.
42 D. W. Davis and D. A. Shirley, Chem. Phys. Lett., 15 (1972) 185.
43 T. H. Lu, T. J. Lee, C. Wong and K. T. Kuo, J. Chinese Chem. Soc., 26 (1979) 53.
44 W. J. Dulmage, W. A. Light, S. J. Marino, C. D. Salzberg, D. L. Smith and W. J. Staudenmayer, J. Appl. Phys., 49 (1978) 5543.
45 R. L. Martin and D. A. Shirley, J. Chem. Phys., 64 (1976) 3685.
46 J. H. Scofield, J. Electron Spectrosc. Relat. Phenom., 8(1976) 129.